Journal of Radioanalytical and Nuclear Chemistry (2024) 333:1073–1082
https://doi.org/10.1007/s10967-023-09346-w

# Naturally occurring radioactive materials (NORM) concentration and health risk assessment of aerosols dust in Nicosia, North Cyprus

**Hesham M. H. Zakaly[1,2] · Akbar Abbasi[3] · Nouf Almousa[4] · Ahmet Savaşan[5]**

Received: 3 July 2023 / Accepted: 23 December 2023 / Published online: 6 February 2024
© The Author(s) 2024


## Abstract

This study was carried out to evaluate the distribution of naturally occurring radioactive materials (NORM) and radiological risk indexes in aerosol dust in Nicosia, Cyprus utilizing a high-resolution HPGe gamma-spectrometry. The activity concentrations of $^{226}$Ra, $^{232}$Th, and $^{40}$K in the selected aerosol dust samples ranged from 25.9–52.4, 21.7–46.3, to 471–1302 Bq kg$^{-1}$, respectively. The average activity concentrations of $^{40}$K were found to be above the Earth's crust average. The internal and external hazard indexes are well below the acceptable limit in most dust samples. All investigated samples met the exemption dose limit of 0.3 mSv y$^{-1}$.


**Keywords** Aerosols dust · Naturally occurring radioactive materials (NORM) · HPGe gamma-spectrometery · Radiological risk

## Introduction

Soil, a significant reservoir for environmental contaminants, consists of various organic and mineral components. As a result, it naturally contains certain levels of radioactive elements, primarily influenced by the parent rock type from which the soil originated. The physicochemical properties of soils further play a crucial role in determining the behavior, concentration, and distribution of radioactive materials within them [1]. Upon inhalation and/or ingestion, these radionuclides emit gamma rays, beta particles, and alpha particles, thereby irradiating the host organism [2]. The presence of natural radionuclides in dust depends on its amount in the origin soil. Also, the origin of dust is mainly related to atmospheric dust, agricultural activities, plant types of the area, soil characteristics, and environmental pollution.

The radiological risk associated is important from the point of view of radiation protection, and some research was reported recently [3–6]. Naturally occurring radioactive materials (NORM) such as $^{40}$K and $^{238}$U, $^{232}$Th, and their decay products that are present in environmental materials such as soil [7, 8], rock [5, 9], water [10–12], and building materials [13–17], can be harmful to human health. Based on the geological formation of the soil, the distribution of radioactivity in soil depends on the type of rock from which it is derived, as well as the nature of its geological composition [18]. Soil not only acts as a source of continuous radiation exposure for humans, but also acts as a means of transporting radioactive materials in the form of dust into the respiratory system [19].

A number of factors influence the distribution of NORM in different geoenvironmental components (e.g., soil, sediment, water, dust), including weathering processes, local geology, and climate conditions [20]. The presence of NORM in sediments or soil is typically related to external radiation exposures if gaseous radon inhalation is not considered. Since exposure to NORM in water involves multiple pathways, these effects are negligible due to the low levels of

✉ Hesham M. H. Zakaly
h.m.zakaly@gmail.com

✉ Akbar Abbasi
akbar.abbasi@kyrenia.edu.tr

1 Physics Department, Faculty of Science, Al-Azhar University, Assiut Branch, Assiut, Egypt

2 Institute of Physics and Technology, Ural Federal University, Ekaterinburg, Russia

3 Faculty of Art and Science, University of Kyrenia, TRNC, Via Mersin 10, Kyrenia, Turkey

4 Department of Physics, College of Science, Princess Nourah Bint Abdulrahman University, P.O. Box 84428, 11671 Riyadh, Saudi Arabia

5 Faculty of Arts and Sciences, Near East University, TRNC, Via Mersin 10, Lefkosa, Turkey

NORM in natural water sources [21]. Unlike the water levels of NORM, the dust levels of NORM cannot be ignored. Additionally, radiation exposures through NORM in dust samples are not limited to external routes (ignoring radon inhalation). The radionuclides contained in dust can enter the lungs through inhalation.

This research was carried out to evaluate the concern of NORM in aerosol dust of the capital city, Nicosia, and assessed the radiological risk indexes in the study area. For this purpose, the NORM concentration, Radium equivalent activity index ($Ra_{eq}$), external hazard indices($H_{ex}$), internal hazard indices ($H_{in}$), and gamma activity concentration index ($I_{\gamma}$) were calculated in the study area.

## Methodology

### Study site

Cyprus, latitude and longitude are 35° 22′ 11.368″ N, 32° 56′ 17.808″ E, and 35° 40′ 11.104″ N, 34° 34′ 40.762″ E, the third-largest island in the Mediterranean Sea. The North section of Cyprus is neighbor of Syria in the East and with Turkey in the North in the Mediterranean Sea. This island has 220 km of length and 90 km of breadth. Cyprus Island is 9251 $km^2$. The capital city of Cyprus, Nicosia, was selected as the study area. A copper mine is located 30 km away from the study area. An ancient Roman slag pile containing copper was found in the western coastal region of the state in 1914, and the company was founded in 1916. When the mining operation was abandoned in 1974, the tailing deposits were exposed to the environment [22].

### Sample collection and preparation

A total of 26 urban dust samples (each weighing over 250 g) have been collected from different locations in the most densely populated district of North Nicosia in order to determine the amount of pollution (Fig. 1). The dustpan and brush used at each sample site were clean, and sampling was conducted with care so that small particles were not disrupted during the process. This study uses a similar method of sampling preparation to those documented in previous studies reported in the literature with the same results [22]. In order to facilitate sample handling, self-sealed polyethylene containers were used to transport samples to the laboratory. Following the drying process, the samples were mechanically sieved and mixed after drying at 80 °C for 48 h. Subsamples were weighed and stored in polyethylene flasks in a cold, dry area until analysis. Because these particles can remain suspended for extended periods of time, they were selected for the study. Another concern associated with fine particles is the increased health risks compared to coarser particles [23]. A sieve of 100 mesh size was used to separate fine particles. The size of those fine particles is between a few microns to 100 microns. The samples were put inside a cylindrical container.

### Measurement and analysis process

In the current study, the levels of NORM in dust samples were determined using the gamma-spectroscopy protocol reported in previous studies [7, 16, 22, 24–28]. Measurements were determined using a High Purity Germanum (HPGe) well detector with 80% efficiency related to the NaI detector, and the sample counting time was 80,000 s per sample. There were three radionuclides identified at the following energies: $^{226}Ra$ (351.9 keV for $^{214}Pb$, 609.2 keV for $^{214}Bi$), $^{232}Th$ (238.6 keV for $^{212}Pb$, 583.1 keV for $^{208}Tl$, 911 keV for $^{228}Ac$) and 1460.83 keV for $^{40}K$. The energy range of approximately 60–1500 keV was calibrated using four standard point sources containing $^{241}Am$, $^{133}Ba$, $^{137}Cs$, and $^{60}Co$. Based on IAEA reference materials RGU-1 (U-ore), RGTh-1 (Th-ore), and RGK-1 ($K_2SO_4$) packed in the same manner as the samples in the same geometry, the spectrometer was calibrated for efficiency over the photon energy range of 186–2700 keV. The quality assurance of measurements was assessed through the analysis of Standard Reference Material IAEA Soil-375 [29]. Data acquisition and analysis were carried out using the GENIE 2000 and Gamma Analysis Software V.3.3, respectively. The following equation was used to determine the minimum detectable activity (MDA) [30] for the detector at a 95% confidence level:

$$MDL\left(\frac{Bq}{kg}\right) = \frac{K_{\alpha} \cdot \sqrt{N_B}}{\eta(E) P_{\gamma} T_C M} \tag{1}$$

where $P_{\gamma}$ is the probability of gamma emission, $K_{\alpha}$ is the statistical coverage factor equal to 1.645, $N_B$ is the background count (cps), $\eta(E)$ is the photo-peak efficiency (dimensionless),$T_C$ is the counting time(s), and M is the sample mass (kg). The Minimum Detectable Activity (MDA) for each of the radionuclides of interest was computed using Eq. (1), resulting in values of 0.50 Bq $kg^{-1}$ for $^{226}Ra$, 0.70 Bq $kg^{-1}$ for $^{232}Th$, and 2.2 Bq $kg^{-1}$ for $^{40}K$.

### Radiological health risks assessment

#### *Radium equivalent activity index ($Ra_{eq}$)*

Naturally, NORM radiation concentrations in surrounding environmental components such as soil, sediments, or dust are not uniform. The "Radium equivalent activity ($Ra_{eq}$)"


**Fig. 1** Geographical location of 26 sampling points in the study area

index is used to remove radionuclide non-uniform activity. This may be calculated using the following Eq. (2):

$$Ra_{eq} = \left( \frac{A_{Ra}}{370} + \frac{A_{Th}}{259} + \frac{A_K}{4810} \right) \times 370 \quad (2)$$

where $A_{Ra}$, $A_{Th}$, and $A_K$ indicate the radioactive concentrations of $^{226}$Ra, $^{232}$Th, and $^{40}$K, respectively. The maximum allowed value of $Ra_{eq}$ was set at 370 Bq kg$^{-1}$ for prospective radiological safety assessment [31].

#### *External & internal hazard indices ($H_{ex}$ & $H_{in}$)*

The external hazard index ($H_{ex}$) can be calculated using Eq. (3) to quantify the externally exposed radiation (ionizing) doses to individual people from dusts. Furthermore, the internal hazard index ($H_{in}$) is used to measure the radiological dangers caused by radon and its products, which can be computed using Eq. (4) [32].

$$H_{ex} = \frac{A_{Ra}}{370} + \frac{A_{Th}}{259} + \frac{A_K}{4810} \le 1 \quad (3)$$

$$H_{in} = \frac{A_{Ra}}{185} + \frac{A_{Th}}{259} + \frac{A_K}{4810} \le 1 \quad (4)$$

where $A_{Th}$, $A_{Ra}$, and $A_K$ represent the radioactivity abundances of radionuclides $^{232}$Th, $^{226}$Ra, and $^{40}$K, respectively. According to UNSCEAR (2000), $H_{ex}$ and $H_{in}$ values should be less than unity in order to minimize the radiation hazard [18].

#### *Gamma activity concentration index (Iγ)*

Gamma activity concentration index (Iγ) can be used to evaluate the risk levels of natural radiation from dusts associated with gamma-emitters. Due to the excessive radiation emitted by surface materials, I was connected with the yearly dose criterion and used as a screening tool to identify substances that could harm human health. $I_\gamma$ can be estimated by Eq. (5) [33, 34]

$$I_\gamma = \frac{A_{Ra}}{150} + \frac{A_{Th}}{100} + \frac{A_K}{1500} \quad (5)$$

where $A_{Ra}$, $A_{Th}$, and $A_K$ are the activity concentrations of $^{226}$Ra, $^{232}$Th, and $^{40}$K (Bq kg$^{-1}$), respectively. The dose criterion of 1 mSv y$^{-1}$ is met for $I \le 6$ [35].

### Statistical analysis

Statistical analysis parameters (Min, Max, Mean, Kurtosis, Skewness) of the radioactivity concentration data were analyzed using Minitab (ver 19) software. Pearson's correlation and principal component analysis (PCA) were applied to investigate the sources of radioactivity concentration in the dust. Also, Cluster analyses were performed to show the similarity of radionuclides and correlation parameters.

## Results and discussion

### Radioactivity concentrations

The measured radioactivity concentrations of NORM in the Nicosia metropolis aerosol dust were presented in Table 1. The activity concentrations of $^{226}$Ra, $^{232}$Th, and $^{40}$K renged from 25.9 ± 3.1 to 52.4 ± 5.3 Bq kg$^{-1}$, 21.7 ± 1.5 to 46.3 ± 3.7 Bq kg$^{-1}$, 471 ± 7 to 1302 ± 22 Bq kg$^{-1}$, respectively. This table also shows the average Earth crust values for the $^{226}$Ra, $^{232}$Th, and $^{40}$K radionuclide concentrations.

The highest mean value was $^{40}$K (787 Bq kg$^{-1}$), and the lowest mean value was $^{232}$Th (31.8 Bq kg$^{-1}$). The mean concentrations of $^{226}$Ra and $^{232}$Th were slightly lower than and higher than the Earth's crust's average background value for soils, respectively. At the same time, the mean concentrations of $^{40}$K exceeded the corresponding background values for soils in Earth's crust [36]. The mean concentrations of $^{226}$Ra, $^{232}$Th, and $^{40}$K measured in dust samples in this study were compared with central Bangladesh dust [37], whereas $^{226}$Ra (86.0 Bq kg$^{-1}$), $^{232}$Th (43.4 Bq kg$^{-1}$) concentrations were higher than and $^{40}$K (448 Bq kg$^{-1}$) concentration lower than the mean concentration of this study. The $^{226}$Ra, $^{232}$Th, and $^{40}$K concentration in dust samples of near gold mining Nyanza, Kenya [38], was reported 27 Bq kg$^{-1}$, 60 Bq kg$^{-1}$, and 112 Bq kg$^{-1}$, respectively. Where $^{232}$Th concentration was reported higher than the $^{226}$Ra and $^{40}$K concentration values were less than the results of this research.

Abbasi et al. [39] measured the concentration of $^{226}$Ra, $^{232}$Th, and $^{40}$K in surface soil samples of the North Cyprus area. The measured concentrations were 83.7 Bq kg$^{-1}$ for $^{226}$Ra, 53.6 Bq kg$^{-1}$ for $^{232}$Th, and 593.9 Bq kg$^{-1}$ for $^{40}$K. The comparison shows that the concentrations of $^{226}$Ra and $^{232}$Th in surface soil samples are higher than those of $^{226}$Ra and $^{232}$Th in dust samples in the same area. On the other hand, the concentration of $^{40}$K in surface soil samples is lower than $^{40}$K concentratiomn in dust samples in the same area. This comparison indicates that Cyprus's source of airborne particles and dust can be an external origin.

The activity concentrations of $^{226}$Ra, $^{232}$Th, and $^{40}$K observed in this study were compared with the surface soil measurements conducted in different parts of the world (Table 2). As shown in Table 2, our average $^{226}$Ra concentrations in dust samples were higher than those measured in China (Baoji) [40], Egypt [41], Greece (Agios Dimitrios) [42], but lower than those in China (Xitulvye) [43], Malaysia (Kedah) [44], Turkey (Kangal) [45], Serbia [46], Nigeria [47], Portugal (Douro) [48], Spain (Velilla) [49], North Cyprus [39], and equal, Bangladesh (Rampal) [50]. Similarly, our average $^{232}$Th activity concentration levels in dust samples were higher than those measured in Turkey (Kangal) [45], Egypt [41], but lower than those in China

**Table 1** The measured radioactivity concentration of NORM (Bq kg$^{-1}$) and radiological health risks in aerosols dust collected from the study area

| Sample | Radioactivity concentration (Bq kg$^{-1}$)* | | | | Radiological health risk | | |
|---|---|---|---|---|---|---|---|
| | $^{226}$Ra | $^{232}$Th | $^{40}$K | Raeq | Hex | Hin | Iγ |
| DS-1 | 26.2 ± 2.7 | 23.5 ± 2.1 | 615 ± 9 | 107.0 | 0.3 | 0.4 | 0.8 |
| DS-2 | 37.8 ± 3.5 | 28.9 ± 2.3 | 753 ± 9 | 137.0 | 0.4 | 0.5 | 1.0 |
| DS-3 | 38.0 ± 3.8 | 31.3 ± 2.8 | 1051 ± 13 | 163.6 | 0.4 | 0.5 | 1.3 |
| DS-4 | 48.5 ± 4.2 | 43.5 ± 3.5 | 1290 ± 16 | 209.9 | 0.6 | 0.7 | 1.6 |
| DS-5 | 31.3 ± 2.6 | 26.0 ± 2.7 | 1302 ± 22 | 168.6 | 0.5 | 0.5 | 1.3 |
| DS-6 | 35.1 ± 3.0 | 29.2 ± 3.0 | 894 ± 12 | 145.5 | 0.4 | 0.5 | 1.1 |
| DS-7 | 28.1 ± 2.8 | 32.0 ± 3.1 | 479 ± 7 | 110.7 | 0.3 | 0.4 | 0.8 |
| DS-8 | 33.4 ± 3.2 | 30.1 ± 3.0 | 815 ± 14 | 139.1 | 0.4 | 0.5 | 1.1 |
| DS-9 | 25.9 ± 3.1 | 28.6 ± 2.9 | 791 ± 13 | 127.6 | 0.3 | 0.4 | 1.0 |
| DS-10 | 27.0 ± 2.2 | 30.4 ± 2.1 | 521 ± 7 | 110.5 | 0.3 | 0.4 | 0.8 |
| DS-11 | 40.7 ± 4.0 | 36.0 ± 3.1 | 598 ± 7 | 138.1 | 0.4 | 0.5 | 1.0 |
| DS-12 | 28.5 ± 2.1 | 31.5 ± 2.2 | 819 ± 13 | 136.5 | 0.4 | 0.4 | 1.1 |
| DS-13 | 52.4 ± 5.3 | 46.3 ± 3.7 | 603 ± 8 | 164.9 | 0.4 | 0.6 | 1.2 |
| DS-14 | 49.3 ± 5.1 | 44.9 ± 3.5 | 921 ± 11 | 184.3 | 0.5 | 0.6 | 1.4 |
| DS-15 | 28.7 ± 2.3 | 31.1 ± 2.6 | 1013 ± 13 | 151.0 | 0.4 | 0.5 | 1.2 |
| DS-16 | 26.4 ± 2.2 | 21.7 ± 1.5 | 471 ± 7 | 93.6 | 0.3 | 0.3 | 0.7 |
| DS-17 | 44.1 ± 3.5 | 35.5 ± 2.9 | 539 ± 8 | 136.3 | 0.4 | 0.5 | 1.0 |
| DS-18 | 30.0 ± 2.7 | 24.8 ± 1.8 | 842 ± 12 | 130.2 | 0.4 | 0.4 | 1.0 |
| DS-19 | 32.6 ± 2.8 | 30.0 ± 2.7 | 636 ± 8 | 124.3 | 0.3 | 0.4 | 0.9 |
| DS-20 | 36.5 ± 3.2 | 32.8 ± 2.9 | 580 ± 10 | 128.0 | 0.3 | 0.4 | 1.0 |
| DS-21 | 32.7 ± 3.0 | 25.6 ± 1.5 | 720 ± 7 | 124.6 | 0.3 | 0.4 | 1.0 |
| DS-22 | 28 ± 2.6 | 27.2 ± 1.8 | 930 ± 11 | 138.4 | 0.4 | 0.4 | 1.1 |
| DS-23 | 38.2 ± 3.5 | 34.5 ± 3.1 | 1019 ± 14 | 165.9 | 0.4 | 0.6 | 1.3 |
| DS-24 | 33.9 ± 3.1 | 31.8 ± 2.8 | 961 ± 12 | 153.2 | 0.4 | 0.5 | 1.2 |
| DS-25 | 34.4 ± 3.7 | 36.9 ± 3.2 | 782 ± 8 | 147.3 | 0.4 | 0.5 | 1.1 |
| DS-26 | 38.1 ± 3.9 | 31.5 ± 3.1 | 517 ± 5 | 122.8 | 0.3 | 0.4 | 0.9 |
| Min–Max | 25.9 ± 3.1–52.4 ± 5.3 | 21.7 ± 1.5–46.3 ± 3.7 | 471 ± 7–1302 ± 22 | 93.6–209.9 | 0.3–0.6 | 0.3–0.7 | 0.7–1.6 |
| Mean | 34.8 | 31.8 | 787 | 140.7 | 0.4 | 0.5 | 1.1 |
| Kurtosis | −0.501 | 0.392 | −0.109 | – | – | – | – |
| Skewness | 0.835 | 0.909 | 0.723 | – | – | – | – |
| Earth's crust average value** | 35 | 30 | 400 | – | – | – | – |

*Uncertainties are given within 1 standard deviation

**(UNSCEAR, 2000b)

(Baoji) [40], China (Xitulvye) [43], Malaysia (Kedah) [44], Serbia [46], Greece (Agios Dimitrios) [42], Portugal (Douro) [48], Spain (Velilla) [49], North Cyprus [39], Bangladesh (Rampal) [50], Nigeria [47]. On the other hand, our average $^{40}$K concentration levels in dust samples were lower than those measured in Portugal (Douro) [48], but higher than those in Turkey (Kangal) [45], Egypt [41], China (Baoji) [40], China (Xitulvye) [43], Malaysia (Kedah) [44], Serbia [46], Greece (Agios Dimitrios) [42], Spain (Velilla) [49], North Cyprus [39], Bangladesh (Rampal) [50], Nigeria [47].

The box plot of $^{226}$Ra, $^{232}$Th, and $^{40}$K activity concentration with mean, individual, and 95th percentile values was presented in Fig. 2. In this Figure, the Earth's crust average values are shown as reference lines to the comparison of this research results.

**Table 2** Comparison of the $^{226}Ra$, $^{232}Th$, and $^{40}K$ concentration results of this study and other studies from different countries with analogical symbol

| Sampling region | Activity concentration ( $Bq\ kg^{-1}$) | | | | | | References |
|---|---|---|---|---|---|---|---|
| | $^{226}Ra$ | Analogy | $^{232}Th$ | Analogy | $^{40}K$ | Analogy | |
| Xitulvye, China | 49.4 | ↑ | 63.5 | ↑ | 396 | ↓ | (Zhang et al., 2017) |
| Baoji, China | 32.1 | ↓ | 49.8 | ↑ | 721 | ↓ | (Dai et al., 2007) |
| Kedah, Malaysia | 102.1 | ↑ | 134 | ↑ | 326 | ↓ | (Alzubaidi et al., 2016) |
| Kangal, Turkey | 37.0 | ↑ | 17.0 | ↓ | 222 | ↓ | (Gören et al., 2017) |
| Serbia | 50.7 | ↑ | 48.6 | ↑ | 560 | ↓ | (Ćujić et al., 2015) |
| Egypt | 14.7 | ↓ | 17.1 | ↓ | 222 | ↓ | (El-Mekawy et al., 2015) |
| Agios Dimitrios, Greece | 26.8 | ↓ | 36.8 | ↑ | 493 | ↓ | (Karamanis et al., 2009) |
| Nigeria | 54.5 | ↑ | 91.1 | ↑ | 287 | ↓ | (Arogunjo et al., 2009) |
| Douro, Portugal | 53.1 | ↑ | 46.3 | ↑ | 845 | ↑ | (Ribeiro et al., 2010) |
| Velilla, Spain | 38.7 | ↑ | 42.9 | ↑ | 445 | ↓ | (Charro et al., 2013) |
| Rampal, Bangladesh | 34.8 | = | 48.9 | ↑ | 719 | ↓ | (Khan et al., 2019) |
| North Cyprus | 83.7 | ↑ | 53.6 | ↑ | 593.9 | ↓ | (Abbasi et al., 2020a) |

## Risk assessment

The $Ra_{eq}$ index, external hazard index ($H_{ex}$), internal hazard index ($H_{in}$), and gamma activity concentration index ($I_{\gamma}$) of all examined samples were presented in Table 1. The $Ra_{eq}$ index, $H_{ex}$, $H_{in}$, and $I_{\gamma}$ ranged from 93.6 to 209.9 with a mean of 141.0, 0.3–0.6 with a mean of 0.4, 0.3–0.7 with a mean of 0.5, 0.7–1.6 with a mean of 1.1, respectively. The maximum value of all four risk indexes was observed in the DS-4 sample. In the DS-4 sample, the Raeq, Hex, Hin, and Iγ index values were 1.49, 1.50, 1.40, and 1.45 times higher than the mean value of the risk indexes in the study area. The DS-4 sampling site is a high-traffic square, which typically refers to a busy urban intersection with a significant vehicular and pedestrian traffic flow. Environmental studies are particularly interested in such areas due to their potential to influence public health and environmental quality. It can be the effect of exhaust pollution and wear and tear of moving car parts. A more detailed analysis would be helpful at the

**Fig. 2** Box-plot of $^{226}$Ra, $^{232}$Th, and $^{40}$K activity concentration in the studied area aerosols dust samples (grey point, circle points, and yellow box mark are represents mean, individual values, and 95th percentile values, respectively). Reference lines of Earth's crust average value shown by dashed lines

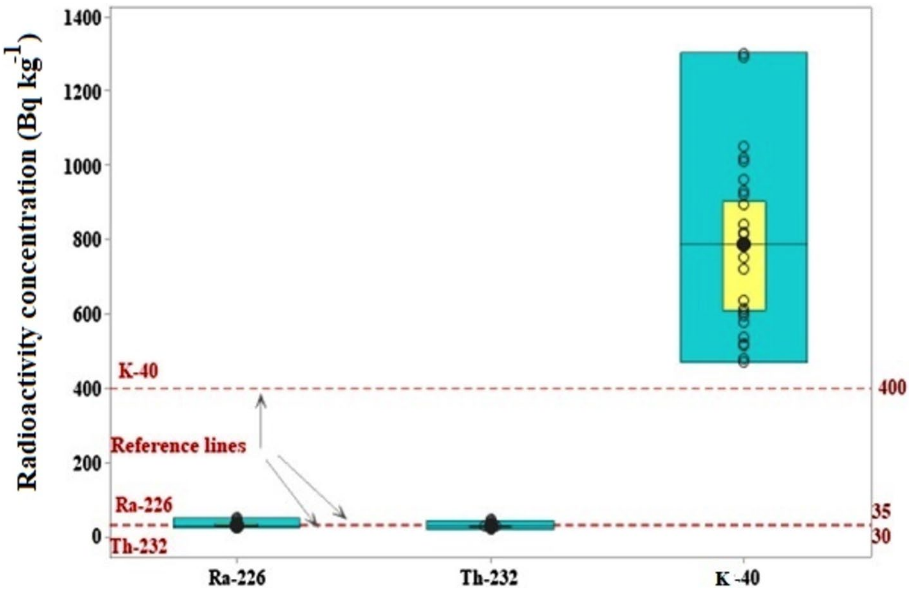


DS-4 site to understand the high concentration of NORM at the DS-4 site.

The minimum value of all four risk indexes was calculated in the DS-16 sample, where this sampling point is a closed area. All the values of $Ra_{eq}$ in the studied samples are found to be lower than the criterion limit of 370 Bq kg$^{-1}$ [51]. The values of the indices ($H_{ex}$ and $H_{in}$) should be < 1. Table 1 shows that the mean values of $H_{ex}$ (0.4) and $H_{in}$ (0.5) are below the criterion value (< 1). The Iγ mean value was calculated under 2, while the dose criterion of 0.3 mSv y$^{-1}$ is met for I $\gamma \leq 2$. This indicated that the annual effective dose due to aerosol dust in the study area was under 0.3 mSv y$^{-1}$. The hot plot of radiological health risk indexes ($Ra_{eq}$, $H_{ex}$, $H_{in}$, and $I_\gamma$) were presented in Fig. 3.

## Statistical assessments

Pearson correlation coefficients were used for $^{226}$Ra, $^{232}$Th, and $^{40}$K activity concentration to create relations in the aerosol dust samples and the resulting correlation matrix is

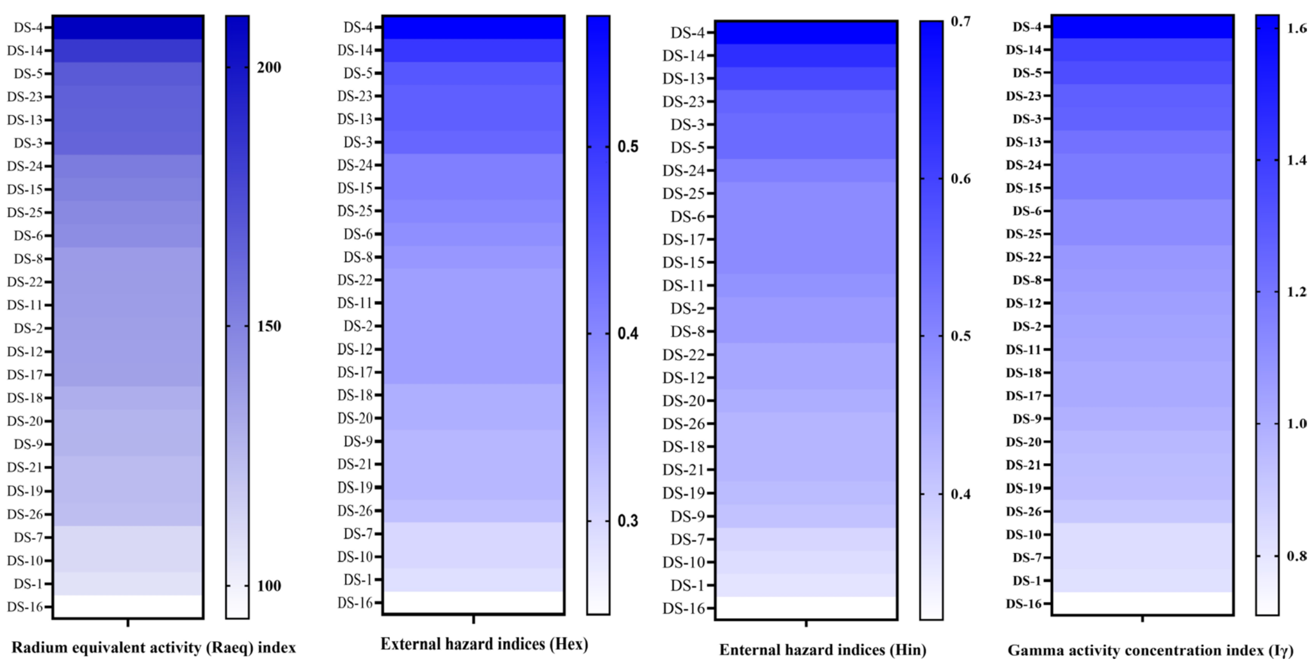


**Fig. 3** Hot plot of radiological health risks indexes ($Ra_{eq}$, $H_{ex}$, $H_{in}$, and $I_\gamma$) in study area

**Table 3** Pearson correlation coefficients between $^{226}$Ra, $^{232}$Th, and $^{40}$K activity concentration values and radiological health risks indexes

| | $^{226}$Ra | $^{232}$Th | $^{40}$K | $Ra_{eq}$ | $H_{ex}$ | $H_{in}$ |
|---|---|---|---|---|---|---|
| $^{226}$Ra | 1 | | | | | |
| $^{232}$Th | 0.854 | 1 | | | | |
| $^{40}$K | 0.148 | 0.135 | 1 | | | |
| $Ra_{eq}$ | 0.691 | 0.689 | 0.795 | 1 | | |
| $H_{ex}$ | 0.691 | 0.689 | 0.795 | 1.000 | 1 | |
| $H_{in}$ | 0.806 | 0.769 | 0.687 | 0.985 | 0.985 | 1 |
| $I_\gamma$ | 0.622 | 0.620 | 0.851 | 0.995 | 0.995 | 0.964 |

*Uncertainties are given within 1 standard deviation

**(UNSCEAR, 2000b)

shown in Table 3. There was a positive correlation among all parameters. Significant correlations ($p < 0.05$) were observed for the pairs $^{226}$Ra and $^{232}$Th (r = 0.854). The Ra and all radiological health risks indexes $Ra_{eq}$ (r = 0.691), $H_{ex}$ (r = 0.691), $H_{in}$ (r = 0.806), and $I_\gamma$ (r = 0.622) show significant correlations. The correlations between $^{40}$K and other two radionuclides ($^{226}$Ra, $^{232}$Th) activity concentrations show no significant correlations.

Cluster analysis was applied to the aerosol dust data to examine the classification of radionuclide groups and radiological health risk indexes to recognize relationships among them. The analysis results are presented as a dendrogram in Fig. 4. The vertical axis represents the similarty percentage of association between the variables, while the greater similarty shows the more significant association. The cluster analysis presents two distinct larger subgroups: the first contains $^{226}$Ra and $^{232}$Th radionuclides, and the second includes $^{40}$K and radiological health risks indexes. The strongest observed association (similarity > 82%) was between $^{40}$K and radiological health risks indexes.

## Conclusion

Twenty-six sampling sites were selected to investigate natural radioactive materials activity concentration in the aerosol dust of Nicosia. The concentration of $^{226}$Ra, $^{232}$Th, and $^{40}$K in aerosol dust was measured. It was found that the average level of $^{226}$Ra, $^{232}$Th in the study area was lower than the Earth's crust average value, while the average value of $^{40}$K radionuclide in aerosols dust was higher than the Earth's crust average value. The radiological health risks indexs were calculated in the study area. The calculated results of radium equivalent activities ($Ra_{eq}$) were lower than the limit of 370 Bq kg$^{-1}$ set by NEA-OECD (Nuclear Energy Agency). The external hazard index ($H_{ex}$), internal hazard index ($H_{in}$), and gamma radiation hazard index ($I_\gamma$) were

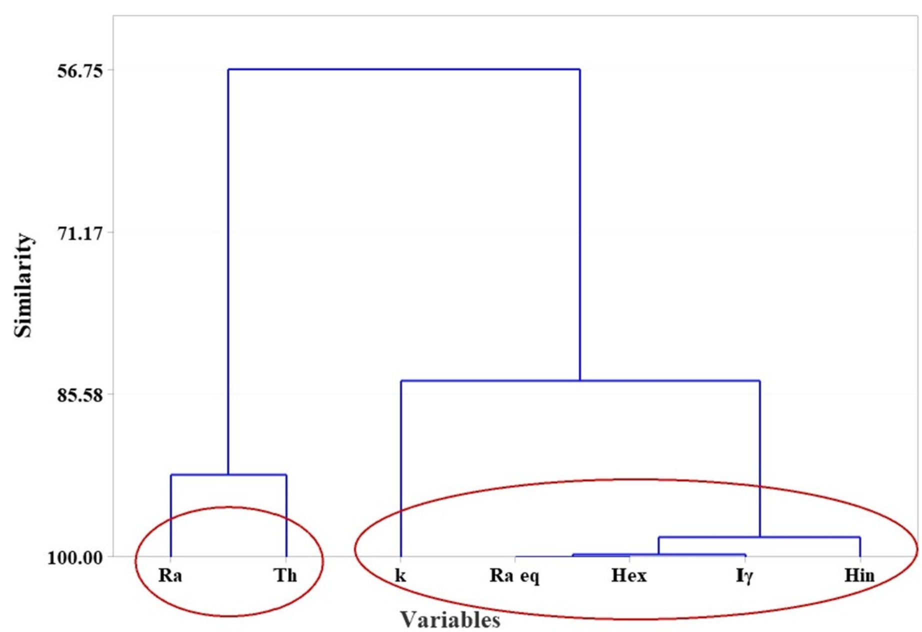


**Fig. 4** Cluster analysis of variables of $^{226}$Ra, $^{232}$Th, and $^{40}$K concentration values with radiological health risks indexes

calculated in all samples. The internal and external hazard indexes were found well below the acceptable limit illustrated by UNSCEAR in all samples. Also, the gamma radiation hazard index ($I_\gamma$) was obtained at less than the met annual effective dose of 0.3 mSv $y^{-1}$. Hence, the radiological risk to human ratio in Nicosia City aerosol dust looks to be negligible.

**Acknowledgements** The author is grateful to Princess Norah bint Abdulrahman University Researchers Supporting Project number (PNURSP2024R111), Princess Nourah bint Abdulrahman University, Riyadh, Saudi Arabia. The research partially funding from the Ministry of Science and Higher Education of the Russian Federation (Ural Federal University Program of Development within the Priority-2030 Program) is gratefully acknowledged.

**Author contributions** H.M.H.Z.: Methodology, Drft preparation, Software, Writing- Original, Writing—Review& Editing. A.A.: Investigation, Conceptualization, Methodology, Software, Project administration, Visualization, Writing—Original draft preparation. N.A.: Methodology, Software, Writing—Review& Editing. Draft. A.S.: Writing—Original draft preparation, Editing.

**Funding** The author is grateful to Princess Norah bint Abdulrahman University Researchers Supporting Project number (PNURSP2024R111), Princess Nourah bint Abdulrahman University, Riyadh, Saudi Arabia.

## Declarations

**Conflict of interest** The authors declare that they have no known competing financial interests or personal relationships that could have appeared to influence the work reported in this paper.

**Open Access** This article is licensed under a Creative Commons Attribution 4.0 International License, which permits use, sharing, adaptation, distribution and reproduction in any medium or format, as long as you give appropriate credit to the original author(s) and the source, provide a link to the Creative Commons licence, and indicate if changes were made. The images or other third party material in this article are included in the article's Creative Commons licence, unless indicated otherwise in a credit line to the material. If material is not included in the article's Creative Commons licence and your intended use is not permitted by statutory regulation or exceeds the permitted use, you will need to obtain permission directly from the copyright holder. To view a copy of this licence, visit http://creativecommons.org/licenses/by/4.0/.

## References

1. Kang T-W, Park W-P, Han Y-U et al (2020) Natural and artificial radioactivity in volcanic ash soils of Jeju Island, Republic of Korea, and assessment of the radiation hazards: importance of soil properties. J Radioanal Nucl Chem 323:1113–1124
2. Anamika K, Mehra R, Malik P (2020) Assessment of radiological impacts of natural radionuclides and radon exhalation rate measured in the soil samples of Himalayan foothills of Uttarakhand, India. J Radioanal Nucl Chem 323:263–274
3. Abbasi A (2023) Bioaccumulation and risk assessment of radiocesium in the Northwest Pacific Ocean from Fukushima Dai-ichi Nuclear Power Plant accident. Mar Pollut Bull 192:114994
4. Abbasi A, Zakaly HMH, Almousa N (2023) Radiotoxic fission products and radiological effects in the Mediterranean Sea biota from a hypothetical accident in Akkuyu Nuclear Power Plant. Mar Pollut Bull 193:115166
5. Abbasi A (2023) Radiation risk assessment of coastal biota from a quasi-Fukushima hypothetical accident in the Mediterranean Sea. Mar Pollut Bull 194:115363. https://doi.org/10.1016/j.marpolbul.2023.115363
6. Abbasi A, Zakaly HMH, Alotaibi BM (2023) Radioactivity concentration and radiological risk assessment of beach sand along the coastline in the Mediterranean Sea. Mar Pollut Bull 195:115527
7. Abbasi A, Mirekhtiary F (2019) $^{137}$Cs and $^{40}$K concentration ratios (CRs) in annual and perennial plants in the Caspian coast. Mar Pollut Bull 146:. https://doi.org/10.1016/j.marpolbul.2019.06.076
8. Abbasi A, Mirekhtiary SF (2019) Risk assessment due to various terrestrial radionuclides concentrations scenarios. Int J Radiat Biol 95:. https://doi.org/10.1080/09553002.2019.1539881
9. Abed NS, Monsif MA, Zakaly HMH et al (2022) Assessing the radiological risks associated with high natural radioactivity of microgranitic rocks: A case study in a northeastern desert of Egypt. Int J Environ Res Public Health 19:473
10. Abbasi A, Mirekhtiary F (2019) Lifetime risk assessment of Radium-226 in drinking water samples. Int J Radiat Res 17:. https://doi.org/10.18869/acadpub.ijrr.17.1.163
11. Abbasi A, Bashiry V (2016) Measurement of radium-226 concentration and dose calculation of drinking water samples in Guilan province of Iran. Int J Radiat Res 14:. https://doi.org/10.18869/acadpub.ijrr.14.4.361
12. Abbasi A, Mirekhtiary F (2017) Gross alpha and beta exposure assessment due to intake of drinking water in Guilan, Iran. J Radioanal Nucl Chem 314:. https://doi.org/10.1007/s10967-017-5493-6
13. Abbasi A (2017) Modeling of lung cancer risk due to radon exhalation of granite stone in dwelling houses. J Cancer Res Ther 13:. https://doi.org/10.4103/0973-1482.204851
14. Abbasi A (2013) Calculation of gamma radiation dose rate and radon concentration due to granites used as building materials in Iran. Radiat Prot Dosimetry 155:. https://doi.org/10.1093/rpd/nct003
15. Abbasi A, Mirekhtiary F (2013) Comparison ofactive and passive methods for radon exhalation from a high-exposure buildingmaterial. Radiat Prot Dosimetry 157:. https://doi.org/10.1093/rpd/nct163
16. Abbasi A, Mirekhtiary F (2013) Comparison of active and passive methods for radon exhalation from a high–exposure building material. Radiat Prot Dosimetry 157:570–574
17. Abbasi A, Hassanzadeh M (2017) Measurement and Monte Carlo simulation of γ-ray dose rate in high-exposure building materials. Nucl Sci Tech 28:. https://doi.org/10.1007/s41365-016-0171-x
18. UNSCEAR (2000) Sources and effects of ionizing radiation: United Nations Scientific Committee on the Effects of Atomic Radiation. UNSCEAR 2000 Rep to Gen Assem 1–10
19. Senthilkumar RD, Narayanaswamy R (2016) Assessment of radiological hazards in the industrial effluent disposed soil with statistical analyses. J Radiat Res Appl Sci 9:449–456
20. Khan R, Haydar MA, Saha S, et al (2022) Spatial distribution and radiological risk quantification of natural radioisotopes in the St. Martin's Island, Bangladesh. In: Soil Health and Environmental Sustainability: Application of Geospatial Technology. Springer, pp 369–388
21. Abedin MJ, Khan R (2022) NORMs distribution in the dust samples from the educational institutions of Megacity Dhaka, Bangladesh: radiological risk assessment. J Hazard Mater Adv 8:100155
22. Abbasi A, Mirekhtiary F, Turhan Ş et al (2022) Spatial distribution and health risk assessment in urban surface soils of Mediterranean Sea region, Cyprus İsland. Arab J Geosci 15:1–11

23. Shilton VF, Booth CA, Smith JP et al (2005) Magnetic properties of urban street dust and their relationship with organic matter content in the West Midlands, UK. Atmos Environ 39:3651–3659
24. Abbasi A, Mirekhtiary F, Mirekhtiary SF (2018) Risk assessment due to various terrestrial radionuclides concentrations scenarios. Int J Radiat Biol 1–22. https://doi.org/10.1080/09553002.2019.1539881
25. Abbasi A, Zakaly HMH, Mirekhtiary F (2020) Baseline levels of natural radionuclides concentration in sediments East coastline of North Cyprus. Mar Pollut Bull 161:111793
26. Abbasi A, Mirekhtiary F (2020) Heavy metals and natural radioactivity concentration in sediments of the Mediterranean Sea coast. Mar Pollut Bull 154:. https://doi.org/10.1016/j.marpolbul.2020.111041
27. Abbasi A (2022) Natural Radiation of Chemical Fertilisers and Radiological Impact on Agriculture Soil. J Radioanal Nucl Chem 331:4111–4118
28. Abbasi A, Algethami M, Bawazeer O, Zakaly HMH (2022) Distribution of natural and anthropogenic radionuclides and associated radiation indices in the Southwestern coastline of Caspian Sea. Mar Pollut Bull 178:113593
29. Asgharizadeh F, Abbasi A, Hochaghani O, Gooya ES (2011) Natural radioactivity in granite stones used as building materials in Iran. Radiat Prot Dosimetry 149:321–326
30. Khandaker MU, Jojo PJ, Kassim HA, Amin YM (2012) Radiometric analysis of construction materials using HPGe gamma-ray spectrometry. Radiat Prot Dosimetry 152:33–37. https://doi.org/10.1093/rpd/ncs145
31. Isinkaye MO, Emelue HU (2015) Natural radioactivity measurements and evaluation of radiological hazards in sediment of Oguta Lake, South East Nigeria. J Radiat Res Appl Sci 8:459–469. https://doi.org/10.1016/j.jrras.2015.05.001
32. Begum M, Khan R, Hossain SM, Al Mamun SMM (2022) Redistributions of NORMs in and around a gas-field (Shabazpur, Bangladesh): radiological risks assessment. J Radioanal Nucl Chem 331:317–330. https://doi.org/10.1007/s10967-021-08107-x
33. Asgharizadeh F, Abbasi A, Hochaghani O, Gooya ES (2012) Natural radioactivity in granite stones used as building materials in Iran. Radiat Prot Dosimetry 149:. https://doi.org/10.1093/rpd/ncr233
34. Kolo MT, Aziz SABA, Khandaker MU et al (2015) Evaluation of radiological risks due to natural radioactivity around Lynas Advanced Material Plant environment, Kuantan, Pahang, Malaysia. Environ Sci Pollut Res 22:13127–13136. https://doi.org/10.1007/s11356-015-4577-5
35. EC ECD-G, Safety N, Protection C, et al (1999) Enhanced Radioactivity of Building Materials. European Communities
36. UNSCEAR (2000) United Nation Scientific Committee on the effects of atomic radiation report to the General Assembly. Vol 1, Annex B Exposures from natural radiation sources
37. Abedin MJ, Khan R (2022) Primordial radionuclides in the dust samples from the educational institutions of central Bangladesh: radiological risk assessment. Heliyon 8:e11446. https://doi.org/10.1016/j.heliyon.2022.e11446
38. Odumo OB, Mustapha AO, Patel JP, Angeyo HK (2011) Radiological survey and assessment of associated activity concentration of the naturally occurring radioactive materials (NORM) in the Migori artisanal gold mining belt of southern Nyanza, Kenya. Appl Radiat Isot 69:912–916. https://doi.org/10.1016/j.apradiso.2011.02.016
39. Abbasi A, Kurnaz A, Turhan Ş, Mirekhtiary F (2020) Radiation hazards and natural radioactivity levels in surface soil samples from dwelling areas of North Cyprus. J Radioanal Nucl Chem 1–8
40. Dai L, Wei H, Wang L (2007) Spatial distribution and risk assessment of radionuclides in soils around a coal-fired power plant: A case study from the city of Baoji, China. Environ Res 104:201–208. https://doi.org/10.1016/j.envres.2006.11.005
41. El-Mekawy AF, Badran HM, Seddeek MK et al (2015) Assessment of elemental and NROM/TENORM hazard potential from non-nuclear industries in North Sinai. Egypt Environ Monit Assess 187:1–21
42. Karamanis D, Ioannides K, Stamoulis K (2009) Environmental assessment of natural radionuclides and heavy metals in waters discharged from a lignite-fired power plant. Fuel 88:2046–2052
43. Zhang T, Bai Y, Hong X et al (2017) Particulate matter and heavy metal deposition on the leaves of Euonymus japonicus during the East Asian monsoon in Beijing. China PLoS One 12:e0179840
44. Alzubaidi G, Hamid F, Abdul Rahman I (2016) Assessment of natural radioactivity levels and radiation hazards in agricultural and virgin soil in the state of Kedah, North of Malaysia. Sci World J 2016:
45. Gören E, Turhan Ş, Kurnaz A et al (2017) Environmental evaluation of natural radioactivity in soil near a lignite-burning power plant in Turkey. Appl Radiat Isot 129:13–18
46. Ćujić M, Dragović S, Đorđević M et al (2015) Radionuclides in the soil around the largest coal-fired power plant in Serbia: radiological hazard, relationship with soil characteristics and spatial distribution. Environ Sci Pollut Res 22:10317–10330
47. Arogunjo AM, Höllriegl V, Giussani A et al (2009) Uranium and thorium in soils, mineral sands, water and food samples in a tin mining area in Nigeria with elevated activity. J Environ Radioact 100:232–240
48. Ribeiro FCA, Silva JIR, Lima ESA et al (2018) Natural radioactivity in soils of the state of Rio de Janeiro (Brazil): Radiological characterization and relationships to geological formation, soil types and soil properties. J Environ Radioact 182:34–43. https://doi.org/10.1016/j.jenvrad.2017.11.017
49. Charro E, Pardo R, Peña V (2013) Chemometric interpretation of vertical profiles of radionuclides in soils near a Spanish coal-fired power plant. Chemosphere 90:488–496
50. Khan R, Das S, Kabir S et al (2019) Evaluation of the elemental distribution in soil samples collected from ship-breaking areas and an adjacent island. J Environ Chem Eng 7:103189
51. NEA/OECD (1979) Exposure to radiation from natural radioactivity in building materials, Report by NEA Group of Experts

**Publisher's Note** Springer Nature remains neutral with regard to jurisdictional claims in published maps and institutional affiliations.